Multipath Entanglement of Two Photons

Alessandro Rossi,[1,*] Giuseppe Vallone,[2,1,3,*] Andrea Chiuri,[1,*] Francesco De Martini,[1,4,*] and Paolo Mataloni[1,3,*]

[1]*Dipartimento di Fisica, Sapienza Università di Roma, Roma 00185, Italy*
[2]*Centro Studi e Ricerche "Enrico Fermi," Via Panisperna 89/A, Compendio del Viminale, Roma 00184, Italy*
[3]*Consorzio Nazionale Interuniversitario per le Scienze Fisiche della Materia, Roma 00185, Italy*
[4]*Accademia Nazionale dei Lincei, via della Lungara 10, Roma 00165, Italy*

(Received 1 December 2008; published 13 April 2009)

We present a novel optical device based on an integrated system of microlenses and single-mode optical fibers. It allows us to collect and direct into many modes two photons generated by spontaneous parametric down-conversion. By this device multiqubit entangled states and/or multilevel qudit states of two photons, encoded in the longitudinal momentum degree of freedom, are created. The multipath photon entanglement realized by this device is expected to find important applications in modern quantum information technology.

DOI: 10.1103/PhysRevLett.102.153902 PACS numbers: 42.65.Lm, 03.67.Bg, 42.50.Dv, 42.79.Ry

Entangling two photons in a high-dimension Hilbert space allows the realization of important quantum information (QI) tasks. These deal with a complete analysis of Bell states [1–3] and novel protocols of superdense coding [4], the possibility to perform secure quantum cryptography [5,6], and a fast, high-fidelity one-way quantum computation [7–11], besides the realization of novel quantum nonlocality tests [12–15].

Multidimensional entangled states of two photons have been realized by engineering both qudit states and hyperentangled (HE) states. In the former each particle belongs to a d-level quantum system, and in the latter the particles are entangled in more than one degree of freedom (DOF). Since a qudit, with $d = 2^N$, is equivalent to N qubits, two-entangled qudits are equivalent to the HE state of two particles entangled in N DOFs. Polarization, time-bin, and spatial entanglement have been adopted to create qudits with $d = 3$ (qutrits) [6,16], $d = 4$ (ququads) [17], and $d = 8$ [18]. At the same time, HE states have been realized by using in different ways polarization, longitudinal momentum, and orbital angular momentum, besides time-bin entanglement [1,19–22].

In this Letter, we present the first experimental realization of a quantum state of two photons entangled in many optical paths. It is based on the spontaneous parametric down-conversion (SPDC) emission of a type I phase-matched nonlinear (NL) crystal operating under the excitation of a continuous wave (cw) laser at wavelength (wl) λ_p. In these conditions, the degenerate signal (s) and idler (i) photons are generated with uniform probability distribution, at wl $\lambda_s = \lambda_i = 2\lambda_p$, over a continuum of correlated $\mathbf{k}$ modes belonging to the lateral surface of a cone. Usually, no more than two correlated spatial modes are used in experiments based on type I crystals; hence, the main part of SPDC radiation is lost. By exploiting the continuum of $\mathbf{k}$-mode emission of type I crystals, high-dimension entangled states can be created [23]. Indeed, a large number of qubits are, in principle, available by this geometry. However, a successful realization of this idea strongly depends on the possibility to overcome the practical difficulties represented by independently collecting and manipulating the SPDC radiation belonging to a large number of $\mathbf{k}$ modes.

By the device realized in this experiment, photon pairs traveling along a large number of $\mathbf{k}$ modes are efficiently coupled into a bundle of single-mode optical fibers by an integrated system of microlenses. Four pairs of correlated $\mathbf{k}$ modes have been selected to generate two maximally entangled ququads, i.e., qudits with $d = 4$ (or equivalently a 4-qubit HE state) encoded in the longitudinal momentum of the photons:

$$|\Psi\rangle_{\mathbf{k}} = \frac{1}{2}\sum_{j=1}^{4} e^{i\phi_j}|j\rangle_A|j\rangle_B, \tag{1}$$

with $|j\rangle_A$ ($|j\rangle_B$) the A (B) photon mode of the jth mode pair and ϕ_j the corresponding phase. Figure 1(a) shows the annular section of the degenerate cone, with four pairs of correlated modes. It is divided in two half-rings, respectively, corresponding to the Alice (A) and Bob (B) side.

This particular geometry allows the creation of multidimensional entangled states. However, it is worth remembering that using an increasing number of $\mathbf{k}$ modes necessarily implies an exponential requirement of resources since this number does not scale linearly with the number of qubits. In fact, 2^N $\mathbf{k}$ modes per photon must be selected within the emission cone to encode N qubits in each photon. On the other hand, since a qudit, with $d = 2^N$, is equivalent to N qubits, the number of modes scales linearly with the size d of the state.

We can relabel for convenience the modes $|1\rangle_A, \ldots, |4\rangle_A$ belonging to the A side as $|E, \ell\rangle_A$, $|I, \ell\rangle_A$, $|I, r\rangle_A$, and $|E, r\rangle_A$, where ℓ (r) and E (I) refer to the left (right) and external (internal) emission modes [see Fig. 1(b)]. They are

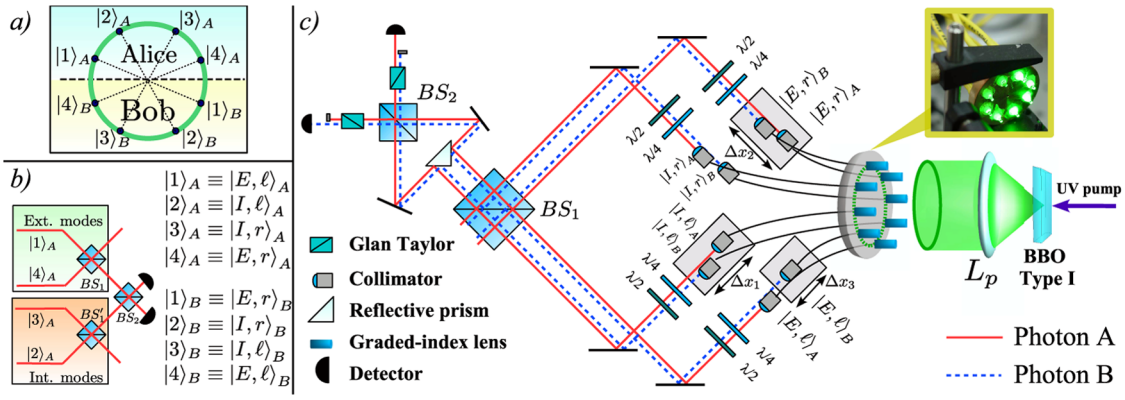

FIG. 1 (color online). (a) Labeling of the correlated pairs of SPDC modes. Photon A (B) can be collected with equal probability into one of the four modes $|1\rangle_j$, $|2\rangle_j$, $|3\rangle_j$, or $|4\rangle_j$ ($j = A, B$), which are relabeled as shown in (b). (b) Scheme needed for measurement of photon A. Here the left (ℓ) and right (r) modes interfere on beam splitters BS_1 and BS_1', while further interference occurs on BS_2 between the external (E) and internal (I) modes. An identical scheme is needed for photon B. (c) Experimental setup: The GL-SMF integrated system injects photon pairs emitted by the crystal into the chained interferometer. The path of photon A (B) is indicated by the continuous red (dashed blue) line. By this scheme, BS_1 plays simultaneously the role of BS_1 and BS_1' on side (b) for both photons. The internal and external modes coming out of the right side of BS_1 interfere on the beam splitter BS_2. Photon A and photon B are separately detected by two single photon counting modules. Micrometric translation stages allow variation of path delays $\Delta x_1, \ldots, \Delta x_3$. Wave plates $\lambda/4$ and $\lambda/2$ enable polarization restoration of photons after SMF transmission. Inset: Picture of the 8 GL-SMF system.

respectively correlated to the B emission modes $|E, r\rangle_B$, $|I, r\rangle_B$, $|I, \ell\rangle_B$, and $|E, \ell\rangle_B$, labeled as $|1\rangle_B, \ldots, |4\rangle_B$ in Fig. 1(a).

In the experiment [cf. Figure 1(c)], a type I 2 mm thick β-barium-borate (BBO) crystal, cut at $\theta = 48°$ and shined by a vertically polarized cw single longitudinal mode MBD-266 Coherent laser ($P = 100$ mW, $\lambda_p = 266$ nm), produces degenerate photon pairs ($\lambda_i = \lambda_s = 532$ nm), with horizontal polarization, along correlated directions belonging to the external surface of a cone. Then a positive lens L_p (focal length $f = 9.5$ cm), located at a distance f from the BBO, transforms the conical emission into a cylindrical one with transverse diameter $D = 12$ mm.

The device collecting SPDC radiation into a set of single-mode fibers consists of an integrated system of 8 graded-index lenses (GLs), regularly spaced along the circumference of the degenerate ring. Each GL [Grintech, model GT-LFRL-100-025-50-NC (532), length = 2.381 mm, diameter = 1.0 mm, numerical aperture = 0.5] was glued to a prealigned single-mode fiber (SMF). We measured a coupling efficiency of almost 60% for each GL-SMF system. Each GL-SMF pair system, corresponding to two correlated $\mathbf{k}$ modes, was then glued in an 8-hole mask, after preliminary optimization of its alignment [cf. the inset in Fig. 1(c)]. In these conditions, for each GL-SMF pair, nearly 7×10^3 coinc/s were measured over a bandwidth $\Delta\lambda = 4.5$ nm, within a coincidence window of 7 ns. This corresponds to a *coincidences/singles* ratio of almost 10%.

By this system, the probability that more than one photon pair excites the entire mode set within the time coincidence window is related to the number of accidental coincidences; hence, it grows quadratically with the number of mode pairs, while the real coincidences increase linearly. This would contribute to reduce the signal to noise ratio if a larger number of mode pairs would be adopted.

The entanglement existing between the four mode pairs was characterized by the interferometric apparatus sketched in Fig. 1(c). For any couple of mode pairs $|i\rangle_A|i\rangle_B$ and $|j\rangle_A|j\rangle_B$ ($i \neq j$), we can define a visibility $V_0^{(ij)} = (C_{ii} + C_{jj} - C_{ji} - C_{ij})/(C_{ii} + C_{jj} + C_{ji} + C_{ij})$, where C_{ab} is the number of coincidences measured between the mode a of photon A and the mode b of photon B. Since almost no coincidence was detected between any pair of noncorrelated modes (such as, for instance, $|1\rangle_A$ and $|2\rangle_B$), we have $V_0^{(ij)} = 0.990 \pm 0.005$ for any couple of mode pairs. Then any positive value of visibility measured in any superposition basis is sufficient to demonstrate the existence of path entanglement for any couple of mode pairs. Similarly, in a 2-qubit entangled state, such as $(1/\sqrt{2})(|0\rangle_A|0\rangle_B + |1\rangle_A|1\rangle_B)$, the entanglement witness $W = \mathbb{1} - \sigma_z^{(A)}\sigma_z^{(B)} - \sigma_x^{(A)}\sigma_x^{(B)}$ [24] reveals the existence of entanglement if the sum of visibilities in the standard basis ($|0\rangle$ and $|1\rangle$) and in the superposition basis $|\pm\rangle = (1/\sqrt{2})(|0\rangle \pm |1\rangle)$ is larger than 1.

Indistinguishability between the four modes on which each photon is emitted can be achieved by the sequence of beam splitters shown in Fig. 1(b). In the actual chained interferometric setup used in the experiment [cf. Fig. 1(c)], the $\mathbf{k}$ modes of photons A or B, corresponding each to a SMF, are matched on the up- and downside of a common 50:50 beam splitter (BS_1), where temporal mode matching is realized by fine adjustment of three optical paths by

spatial delays Δx_1, Δx_2, and Δx_3. Precisely, on the Alice side, left modes $|I, \ell\rangle_A$ and $|E, \ell\rangle_A$ interfere with the corresponding right modes $|I, r\rangle_A$ and $|E, r\rangle_A$. The same happens with the corresponding Bob side modes. The interference on BS_1 derives from spatial and temporal indistinguishability obtained by independent adjustment of delays Δx_1 and Δx_3, for the internal and external mode sets, respectively. This operation acts as a measurement on the $\ell - r$ qubit since the BS_1 output modes are, respectively, $(1/\sqrt{2})(|\ell\rangle_j \pm e^{i\alpha_j}|r\rangle_j)$ $(j = A, B)$, regardless of the value of the $E - I$ qubit.

Interference between internal and external modes is the necessary step to test the existence of path entanglement over the entire set of **k** modes. This was performed by creating interference on the second beam splitter BS_2, i.e., by making indistinguishable the four events $|1\rangle_A|1\rangle_B$, $|2\rangle_A|2\rangle_B$, $|3\rangle_A|3\rangle_B$, and $|4\rangle_A|4\rangle_B$. Hence, interference can be observed between the output modes of BS_1, i.e., by spatial superposition of the I and E modes on BS_2. Let us consider the input ports of the 50:50 beam splitter BS_2 in Fig. 1(c). There are two interfering modes for the Alice and two for the Bob side, coming one from the internal and the other from the external side of the first interferometer. Thus, temporal indistinguishability on BS_2 is obtained by varying path delay of the I modes with respect to the E modes. This can be achieved by simultaneously varying Δx_2 and Δx_3. Precisely, for any $\Delta x_2 = \delta L$ and $\Delta x_3 = 2\delta L$ (with $\delta L/c$ lower than the pump coherence time), we kept at the same time the interference of the external modes on BS_1 and varied the delay of the external mode with respect to the internal modes on BS_2. In this way, we were able to simultaneously achieve interference on both BS_1 and BS_2. In the experiment, phase stability could be achieved by mechanical stabilization of the interferometric setup and by thermal heating of the fiber system. All of the measurements presented in this Letter were performed without temperature stabilization of the fiber apparatus.

The interference patterns given in Figs. 2(a) and 2(b), obtained by varying Δx_1 and Δx_3, respectively, demonstrate the existence of path entanglement (on BS_1), for both the internal and external modes. As already explained [19], when the delay is simultaneously changed for two modes [as it happens by changing Δx_1 for the internal modes in Fig. 2(a)], the state phase is self-stabilized (in this case, it is almost equal to π). This is evident in Fig. 2(a), where the small asymmetries come from small temperature fluctuations. On the other hand, by changing only one path, as done by varying Δx_3 in Fig. 2(b) [or Δx_2 in Fig. 2(c)], phase fluctuates randomly. For the same reason, the FWHM of the interference pattern of Fig. 2(b) [and 2(c)] doubles the one of Fig. 2(a).

The two experimental results (with visibilities $V = 0.73 \pm 0.02$ and $V = 0.80 \pm 0.02$) demonstrate the entanglement for the internal [Fig. 2(a)] and external [Fig. 2(b)] modes separately. The presence of a multipath entanglement over the entire set of modes is demonstrated by the third interference pattern of Fig. 2(c) ($V = 0.78 \pm 0.02$) occurring on BS_2 between $|I, \ell\rangle_A|I, r\rangle_B$ and $|E, \ell\rangle_A|E, r\rangle_B$ and obtained by varying Δx_2. All of the visibilities (here and in the following) were measured by setting $\Delta x_i = 0$ and observing coincidences varying by thermal phase fluctuations. The maximum and minimum values, corresponding to $\phi = \pi$ and $\phi = 0$, respectively, allow one to calculate the visibility.

As a further demonstration of multipath entanglement, we compare in Fig. 3 the coincidence oscillations obtained for different values of delays Δx_1, Δx_2, and Δx_3. In these measurements, the phase was almost constant within each data acquisition (1 s) but varied randomly due to temperature fluctuations from acquisition to acquisition. The first two oscillations correspond to independent interference of the internal ($V = 0.65 \pm 0.02$) and external ($V = 0.67 \pm 0.02$) modes on BS_1. The third oscillation corresponds to the coincidences measured in conditions of no temporal interference on BS_2 (i.e., by setting $\Delta x_1 = \Delta x_3 = 0$ and $\Delta x_2 \neq 0$). This must be compared with the fourth oscillation data, obtained when $\Delta x_1 = \Delta x_2 = \Delta x_3 = 0$, that clearly show the enhancement of signal due to the complete indistinguishability of the four pairs of modes caused by multipath entanglement. The upper bound of coincidence counts (1130), compared to the maximum that can be obtained in the absence of interference (660), corresponds to a total visibility $V = 0.71 \pm 0.02$. This result is the signature of the entanglement existing between the four pairs of modes.

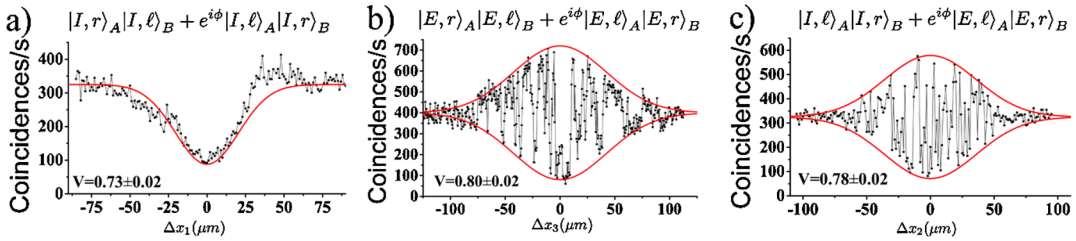

FIG. 2 (color online). Interference patterns obtained by spatial superposition of the (a) internal and (b) external modes on BS_1 as a function of delays Δx_1 and Δx_3. (c) "Hybrid" interference condition obtained, varying Δx_2, by spatial superposition on BS_2 of internal and external modes. Each solid (red) line has been drawn by using the value of visibility measured at $\Delta x_i = 0$ (see text).

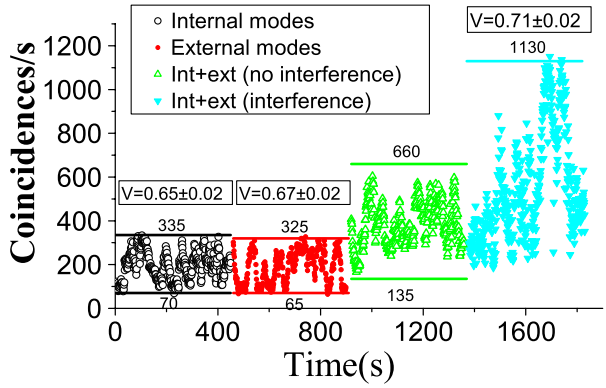

FIG. 3 (color online). Coincidence count oscillations demonstrating multipath entanglement. The first two traces correspond to interference occurring on BS_1 of internal and external modes, separately. The third trace refers to the whole set of mode pairs when no interference occurs on BS_2 (i.e., for $\Delta x_1 = \Delta x_3 = 0$ and $\Delta x_2 \neq 0$). Here the upper (660) and lower (135) bound are given by the sum of maxima and minima, respectively, of the first two traces. In the last trace, coincidences are measured in conditions of complete mode interference ($\Delta x_1 = \Delta x_2 = \Delta x_3 = 0$).

In conclusion, we presented in this Letter the first experimental realization of a multipath entanglement of two photons. The experiment was performed by collecting four pairs of correlated modes of the degenerate SPDC radiation emitted by a NL crystal cut for type I phase matching. To this purpose, we successfully realized an integrated system of eight graded-index lenses coupled to a corresponding set of single-mode optical fibers. We tested the entanglement generated over the entire SPDC conical emission of the crystal by using an especially developed chained multipath interferometer.

The novel device presented in this Letter can be extended to an even larger number of **k** modes by exploiting the continuum emission of the crystal and used together with an integrated optical circuit to realize miniaturized quantum optical networks of increasing complexity [25].

Besides multiqubit entanglement, this system can be successfully used in other QI processes. As an example, it can be adopted in the realization of a "quasideterministic" source of heralded single photons emitted along one-half of the SPDC modes and triggered by the photons emitted along the other half of correlated modes [26]. The same device allows the efficient multiplexing transmission to many pairs of users and over long fiber distances of time-bin entanglement, which is not affected by thermal or mechanical fiber instabilities [27].

This device is a useful tool for an efficient generation and distribution of entanglement since it allows one to maximize the emission of photon pairs for a given value of the pump power. Other configurations can be used for this purpose, for instance, those based on a sequence of mirrors and beam splitters or several nonlinear crystals, but at the price of a strong reduction of SPDC coincidences.

*http://quantumoptics.phys.uniroma1.it/

[1] C. Schuck, G. Huber, C. Kurtsiefer, and H. Weinfurter, Phys. Rev. Lett. **96**, 190501 (2006).
[2] M. Barbieri, G. Vallone, P. Mataloni, and F. De Martini, Phys. Rev. A **75**, 042317 (2007).
[3] T.-C. Wei, J. T. Barreiro, and P. G. Kwiat, Phys. Rev. A **75**, 060305(R) (2007).
[4] J. T. Barreiro, T.-C. Wei, and P. G. Kwiat, Nature Phys. **4**, 282 (2008).
[5] H. Bechmann-Pasquinucci and A. Peres, Phys. Rev. Lett. **85**, 3313 (2000).
[6] R. Thew, A. Acin, H. Zbinden, and N. Gisin, Quantum Inf. Comput. **4**, 93 (2004).
[7] H. J. Briegel and R. Raussendorf, Phys. Rev. Lett. **86**, 910 (2001); R. Raussendorf and H. J. Briegel, *ibid.* **86**, 5188 (2001).
[8] G. Vallone, E. Pomarico, P. Mataloni, F. De Martini, and V. Berardi, Phys. Rev. Lett. **98**, 180502 (2007).
[9] K. Chen *et al.*, Phys. Rev. Lett. **99**, 120503 (2007).
[10] G. Vallone, E. Pomarico, F. De Martini, and P. Mataloni, Phys. Rev. Lett. **100**, 160502 (2008).
[11] G. Vallone, E. Pomarico, F. De Martini, and P. Mataloni, Laser Phys. Lett. **5**, 398 (2008).
[12] D. Collins, N. Gisin, N. Linden, S. Massar, and S. Popescu, Phys. Rev. Lett. **88**, 040404 (2002).
[13] M. Barbieri, F. De Martini, P. Mataloni, G. Vallone, and A. Cabello, Phys. Rev. Lett. **97**, 140407 (2006).
[14] D. Kaszlikowski, P. Gnaciński, M. Żukowski, W. Miklaszewski, and A. Zeilinger, Phys. Rev. Lett. **85**, 4418 (2000).
[15] T. Yang *et al.*, Phys. Rev. Lett. **95**, 240406 (2005).
[16] G. Vallone, E. Pomarico, F. De Martini, P. Mataloni, and M. Barbieri, Phys. Rev. A **76**, 012319 (2007).
[17] E. V. Moreva, G. A. Maslennikov, S. S. Straupe, and S. P. Kulik, Phys. Rev. Lett. **97**, 023602 (2006).
[18] L. Neves *et al.*, Phys. Rev. Lett. **94**, 100501 (2005).
[19] M. Barbieri, C. Cinelli, P. Mataloni, and F. De Martini, Phys. Rev. A **72**, 052110 (2005).
[20] J. T. Barreiro, N. K. Langford, N. A. Peters, and P. G. Kwiat, Phys. Rev. Lett. **95**, 260501 (2005).
[21] C. Cinelli, M. Barbieri, R. Perris, P. Mataloni, and F. De Martini, Phys. Rev. Lett. **95**, 240405 (2005).
[22] W.-B. Gao *et al.*, arXiv:0809.4277.
[23] M. Żukowski, A. Zeilinger, and M. A. Horne, Phys. Rev. A **55**, 2564 (1997).
[24] G. Tóth and O. Gühne, Phys. Rev. Lett. **94**, 060501 (2005).
[25] A. Politi, M. J. Cryan, J. G. Rarity, S. Yu, and J. L. O'Brien, Science **320**, 646 (2008).
[26] A. L. Migdall, D. Branning, and S. Castelletto, Phys. Rev. A **66**, 053805 (2002).
[27] J. Brendel, N. Gisin, W. Tittel, and H. Zbinden, Phys. Rev. Lett. **82**, 2594 (1999).